Quantitative ATR-IR Analysis of Anisotropic Polymer Films: Extraction of Optical Constants

Kiril R. Kirov and Hazel E. Assender*

Department of Materials, University of Oxford, Parks Road, Oxford OX1 3PH, U.K.

Received July 7, 2003

ABSTRACT: In a series of three papers we present the results of surface structure analysis of anisotropic polymer films using ATR-IR spectroscopy. In the first paper, the methodology for quantitative ATR-IR analysis of optically biaxial polymer films of orthorhombic symmetry is outlined, and results are presented of the first stage of the analysis—the extraction of the anisotropic optical constants of the films. Attention is drawn to the necessity that adequate sample/ATR-IR crystal contact is achieved in order to measure the correct reflectivity spectra of the sample/crystal interface and therefore obtain the correct (n, k) spectra of the analyzed film. The anisotropic absorption index spectra of PET and isotactic polypropylene films are presented in the 1800−670 and 1400−800 cm^{-1} range, respectively, along with the ATR-IR spectra from which the optical constants have been calculated. The extraction of all three principal absorption index spectra of PET films allowed us to examine the optical anisotropy of PET films formed by uniaxial-planar and biaxial drawing. The uniaxial-planar films are strongly optically biaxial, whereas the biaxially drawn films have similar properties in the film plane, which are very different from those along the film thickness direction. These differences in optical anisotropy are related to the difference in chain orientation induced during uniaxial-planar and biaxial deformation of PET films and to the anisotropy of the PET monomer unit.

Introduction

Polymer films manufactured via the flat-film production process owe their successful application in a broad range of areas to the significant practical and scientific understanding of the processes occurring during their production. In essence, polymer flat-film formation is centered on controlling the microstructure that develops during stretching of an initially amorphous polymeric material. In most cases the interest is in producing films with a high degree of chain orientation and crystallinity in order to achieve a desirable set of mechanical and optical properties and good dimensional stability of the final film. Thus, strain-induced molecular orientation and crystallization phenomena are at the core of any polymer film production process.

While the structural rearrangement occurring in the material during film production has been extensively studied for the bulk, their surface structure has remained largely unexplored. It is therefore interesting from a scientific point of view to obtain a more detailed picture of the spatial variation of microstructure in polymer films and of the factors that control it. The scientific interest is further corroborated by the ever-growing application of polymer films in composite materials in which the polymeric material serves as a substrate, the surfaces of which are coated with organic or inorganic layers. In such materials the properties both required and produced close to the surface of the film could be very different from those of the bulk. There is therefore strong practical impetus toward gaining further knowledge of surface structure formation in polymer films.

In a series of papers we present the results of the application of attenuated total reflection infrared (ATR-IR) spectroscopy to the analysis of the surface structure of polymer films prepared via the flat-film production process. This, the first paper of the series is devoted to outlining the methodology for quantitative ATR-IR analysis of anisotropic polymer films and providing examples of its implementation in the analysis of two commercially important polymers—poly(ethylene terephthalate) (PET) and polypropylene (PP). The methodology is based on existing theoretical treatments of propagation of light in anisotropic media. It has two main stages: the extraction of the optical constants of the analyzed film from the measured ATR-IR spectra and band intensity analysis of the derived absorption index k and absorption coefficient K spectra of the material. The present paper focuses on the first stage of the analysis—the extraction of optical constants. The analysis of the surface structure of a commercial PET film and surface structure formation during drawing of amorphous PET are the subject of the following papers of the series.

Theory

Elements of Optics. Light propagating across the plane boundary between two isotropic nonabsorbing media is divided into a reflected and a refracted wave (Figure 1). The fractions of incident light reflected and transmitted at the boundary, termed reflectivity (R) and transmissivity (T), respectively, are given by the following expressions:[1]

$$R_\perp = |r_\perp|^2 = \frac{|R_\perp|^2}{|A_\perp|^2}, \quad T_\perp = \frac{n_2}{n_1}\frac{\cos\theta_t}{\cos\theta_i}|t_\perp|^2 = \frac{n_2}{n_1}\frac{\cos\theta_t}{\cos\theta_i}\frac{|T_\perp|^2}{|A_\perp|^2}$$

$$R_\parallel = |r_\parallel|^2 = \frac{|R_\parallel|^2}{|A_\parallel|^2}, \quad T_\parallel = \frac{n_2}{n_1}\frac{\cos\theta_t}{\cos\theta_i}|t_\parallel|^2 = \frac{n_2}{n_1}\frac{\cos\theta_t}{\cos\theta_i}\frac{|T_\parallel|^2}{|A_\parallel|^2|} \quad (1)$$

In eq 1 $\parallel$ and $\perp$ denote light polarization parallel and perpendicular to the plane of incidence, A and T denote

* Corresponding author: Tel +44-(0)1865-273781; Fax +44-(0)-1865-273789, e-mail hazel.assender@materials.ox.ac.uk.

10.1021/ma030369j CCC: $27.50
Published on Web 01/06/2004

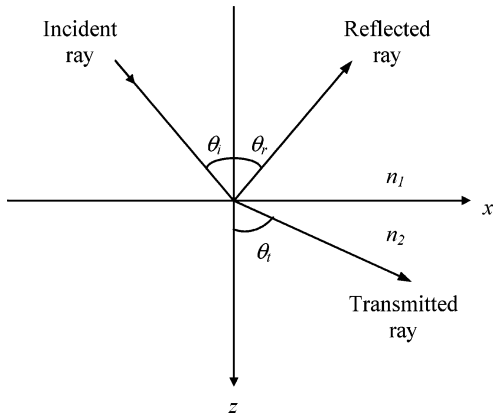

Figure 1. Reflection and refraction of light at a plane boundary between two homogeneous isotropic media of refractive indices n_1 and n_2. The plane of incidence is *Oxz*; the angles of incidence, reflection, and refraction are denoted as θ_i, θ_r, and θ_t, respectively.

the amplitude of the incident and transmitted wave, n_1 and n_2 are the refractive indices of the two media, and θ_i and θ_t are the angles of incidence and refraction. The parallel and perpendicular polarizations are also commonly denoted with the symbols p and s, respectively. The amplitude reflection and transmission coefficients of the interface $r_{\perp,||}$ and $t_{\perp,||}$ are determined by the optical properties of the two media as follows:[1−3]

$$r_\perp = \frac{R_\perp}{A_\perp} = \frac{n_1 \cos\theta_i - n_2 \cos\theta_t}{n_1 \cos\theta_i + n_2 \cos\theta_t}, \qquad r_{||} = \frac{R_{||}}{A_{||}} = \frac{n_2 \cos\theta_i - n_1 \cos\theta_t}{n_2 \cos\theta_i + n_1 \cos\theta_t} \quad (2)$$

$$t_\perp = \frac{T_\perp}{A_\perp} = \frac{2n_1 \cos\theta_i}{n_1 \cos\theta_i + n_2 \cos\theta_t}, \qquad t_{||} = \frac{T_{||}}{A_{||}} = \frac{2n_1 \cos\theta_i}{n_2 \cos\theta_i + n_1 \cos\theta_t} \quad (3)$$

When light is incident on the boundary between two nonabsorbing media from the medium of higher refractive index ($n_2/n_1 < 1$) at angles of incidence θ_i greater than a critical value θ_c ($\sin\theta_c = n_2/n_1$), it undergoes what is termed total internal reflection—there is no lasting flow of energy into the second medium despite the fact that the electromagnetic field in this medium is not discontinued.[1] Using a complex notation, the electric field vector of the transmitted wave $\mathbf{E}_t$ in total internal reflection can be written in terms of the coordinates of Figure 1 as[3]

$$\mathbf{E}_t = \mathbf{E}_t^0 e^{-\alpha z} e^{i(kx\sin\theta_t - \omega t)} \quad (4)$$

where

$$\alpha = k\sqrt{\frac{n_1^2 \sin^2\theta_i}{n_2^2} - 1} \quad (5)$$

In eq 4, $\mathbf{E}_t^0$ represents the direction and maximum amplitude of $\mathbf{E}_t$, $k = |\mathbf{k}| = 2\pi/\lambda$ is the amplitude of the wave vector $\mathbf{k}$, ω is the circular frequency, and t is time. From eqs 4 and 5 it is evident that at angles of incidence $\theta_i > \theta_c$ the transmitted wave diminishes exponentially with distance from the boundary into the second medium.

For absorbing nonmagnetic media eqs 1−5 remain valid with the substitution of the real refractive index with a complex refractive index[2]

$$\hat{n} = \sqrt{\hat{\epsilon}} = n + ik \quad (6)$$

where $\hat{\epsilon}$ is the complex dielectric constant of the medium. The quantity k in (6) is termed the absorption index of the medium and is a measure of the attenuation of the wave per unit path length in the medium. The substitution of n_2 with n_2 in (4) and (5) implies that in internal reflection at angles of incidence greater than θ_c the attenuation of the transmitted wave has an additional contribution due to absorption by the medium. As a consequence of the absorption by the second medium, the time average of the energy flow across the boundary is different than zero, and the reflection is therefore termed attenuated total reflection.[1]

Light propagation is further complicated in anisotropic materials where the electromagnetic anisotropy of optical media must be described with second rank tensors. In terms of their anisotropy with respect to electromagnetic waves optical media are classified as isotropic ($\hat{\epsilon}_x = \hat{\epsilon}_y = \hat{\epsilon}_z$), uniaxial ($\hat{\epsilon}_x = \hat{\epsilon}_y \neq \hat{\epsilon}_z$), and biaxial ($\hat{\epsilon}_x \neq \hat{\epsilon}_y \neq \hat{\epsilon}_z$), ϵ_j ($j = x, y, z$) being the principal components of the complex dielectric constant tensor.[4] The propagation of a plane wave across the boundary between an isotropic and an arbitrarily oriented with respect to the boundary optically biaxial medium of orthorhombic or higher symmetry leads to the formation of two refracted waves in the biaxial medium. In the general case both refracted waves are extraordinary;[4] e.g., their velocities depend on the direction of propagation. However, reflection and refraction become simpler when the plane of incidence coincides with one of the principal planes, and the surface of discontinuity is normal to that plane. Under such conditions s-polarized light entering the anisotropic medium produces ordinary waves only, and p-polarized light produces extraordinary waves only.[5] The velocity of the ordinary wave is independent of the propagation direction, and it travels like in an isotropic medium.[5,6] Assuming light incidence in the principal *Oxz* plane toward the interface between an isotropic nonabsorbing and an anisotropic absorbing medium that contains the principal *Oxy* plane of the anisotropic medium, the amplitude reflection coefficients of the interface take the form[6]

$$r_\perp = \frac{n_1 \cos\theta_i - (\hat{n}_y^2 - n_1^2 \sin^2\theta_i)^{1/2}}{n_1 \cos\theta_i + (\hat{n}_y\hat{n}_2 - n_1^2 \sin^2\theta_i)^{1/2}} \quad (7)$$

$$r_{||} = \frac{\hat{n}_x n_z \cos\theta_i - (\hat{n}_z^2 - n_1^2 \sin^2\theta_i)^{1/2}}{\hat{n}_x\hat{n}_z \cos\theta_i + (\hat{n}_z^2 - n_1^2 \sin^2\theta_i)^{1/2}} \quad (8)$$

Basis of Quantitative Infrared Analysis. As shown above, neither the reflectivity R nor the transmissivity T (the quantities measurable in an IR experiment) is a sole function of the absorption properties of the medium. Quantitative infrared spectroscopy analysis therefore requires as a first step the extraction from R or T of the optical constants (n, k) of the analyzed medium. The absorption index k is used to calculate the absorption

coefficient K of the medium:

$$K = 4\pi\nu k \tag{9}$$

which accounts for the decrease of light intensity due to absorption by the medium via the relation

$$I = I_0 e^{-Kl} \tag{10}$$

The intensity of peaks in the K spectrum can then be used for concentration analysis by application of Beer's law

$$A = Kl = acl \tag{11}$$

where A is the absorbance of the medium, l is the path length of light in the medium, c is the concentration of absorbing species, and a is Beer's absorption coefficient. In eq 11 we have deliberately omitted expressing the absorbance as $-\log(I/I_0)$ because we are making a clear distinction between the true absorption of the medium (Kl) and the widely used approximation.

Experimental Section

Materials. The following films were used for ATR-IR analysis: a commercial biaxially drawn PET film of thickness 12 μm, here referred to as the PET-T film; an amorphous PET film (PET-D) stretched to a draw ratio $\lambda = 3.4$ on an Instron 4204 machine at a temperature of 80 °C and at a rate of 0.013 s^{-1}; a commercial oriented polypropylene film (OPP) of thickness 20 μm. A 1.5 μm thick PET film supplied by GoodFellow (PET-G) was used for transmission infrared analysis.

Optical Microscopy. A Leitz Wetzlar microscope equipped with a polarizer and an analyzer was used to determine the direction of the principal optic axes in the analyzed films.

Refractive Index Measurements. The principal refractive indices of the polymer films were measured using an Abbe refractometer equipped with a polarizing eyepiece at the wavelength of the sodium D line ($\lambda = 589.6$ nm). An immersion liquid of high refractive index ($n_D^{25°} = 1.7300$) was used in order to ensure good contact between the analyzed films and the prism of the refractometer. All measurements were performed at 23 ± 2 °C.

Infrared Spectroscopy. Infrared spectroscopy was performed on a Perkin-Elmer Spectrum 2000 Explorer FTIR spectrometer. All measurements were made with s- and p-polarized light at a wavenumber resolution of 4 cm^{-1}. Light polarization was achieved using a KRS-5 wire grid polarizer with an efficiency of 95% at 2000 cm^{-1}.

The ATR-IR spectra of the polymer films were acquired using a variable angle multipurpose reflection accessory Seagull (Harrick Scientific Corp.) equipped with a rotating hemispherical internal reflection element (IRE). All ATR-IR measurements were done in the 4000−650 cm^{-1} region while purging the sample compartment with nitrogen. The use of a rotating hemispherical crystal allowed polarized light ATR-IR spectra of the oriented films to be acquired along their principal optic axes without breaking the sample/ATR crystal contact.

Transmission measurements in the 4000−370 cm^{-1} region were made at an angle of 30° from the film normal using a Brewster angle attachment purchased from Harrick Scientific Corp.

Programming. The optical constants of the analyzed films were calculated in the 1800−680 cm^{-1} region using MATLAB.

Results and Discussion

Methodology for Quantitative Infrared Analysis of Polymer Films Produced via the Flat-Film Formation Process. The flat-film production of polymer films typically involves the formation of an amorphous precursor film by rapid melt quenching followed by sequential or simultaneous biaxial drawing in two mutually orthogonal directions. During the deformation the chains of the polymer become preferentially aligned parallel to the drawing direction. The optical properties of the polymer film therefore change continuously throughout the process of flat-film formation—while the precursor is to a good approximation optically isotropic, the stretched films can be expected to be optically uniaxial or biaxial. Since biaxial drawing is carried out in two mutually orthogonal directions, polymer films formed via this method are bound to possess at least orthorhombic symmetry in their optical properties. It is therefore possible to take advantage in spectroscopic experiments of the simplified propagation of light along the principal planes of orthorhombic anisotropic media. Thus, in accord with eq 7, three s-polarized light measurements along the principal optical planes of a polymer film are in general sufficient to extract its principal optical constants. Because of the finite thickness of polymer films, however, two measurements with s-polarized light and one with p-polarized light must be made in order to extract all principal optical constant components (eqs 7 and 8). This is the approach used throughout this work (Figure 2). Unless otherwise stated, the axis of drawing (machine direction, MD) or preferred film orientation is here denoted as the x axis, the y axis corresponds to the direction lying in the plane of the film normal to the x axis (transverse direction, TD), and the z axis coincides with the film thickness or normal direction (ND).

Program Validation and Extraction of Optical Constants from Experimental Data. The extraction of optical constants from ATR-IR spectra was performed using Kramers−Kronig (KK) analysis due to its universality, computational simplicity, and speed. The Kramers−Kronig equations have the following form:[7]

$$n(\omega') = n_\infty + \frac{2}{\pi}\mathbf{P}\int_0^\infty \frac{\omega k(\omega)}{\omega^2 - \omega'^2}\,d\omega$$

$$k(\omega') = -\frac{2\omega}{\pi}\mathbf{P}\int_0^\infty \frac{n(\omega)}{\omega^2 - \omega'^2}\,d\omega \tag{12}$$

where **P** denotes the principal value of the integral. Equations 12 include the term $n_{2\infty}$—the refractive index of the material in a nonabsorbing spectral region. For the purposes of this work we used the refractive indices measured with an Abbe refractometer as described in the Experimental Section.

The code for extraction of optical constants was validated using simulated ATR-IR spectra in a manner similar to the one used previously for isotropic media.[8−11] Virtual optical constant spectra were calculated using a Lorentzian type harmonic oscillator function suggested by Ohta and Ishida[9] and used to calculate the model ATR-IR spectra that were subjected to the KK analysis. Figure 3 shows an example of a set of model optical constants of an anisotropic absorbing medium (top row) and the results of the KK calculations performed on the model ATR-IR spectrum in the middle and bottom rows. Comparison of the model and the derived out-of-plane optical constant spectra of that figure confirms that the KK calculation has returned the correct values of k_{2z} and n_{2z}. In addition, the bottom row of Figure 3 where the model and the calculated reflectivity curves are overlaid shows that there is an excellent fit to the model spectrum.

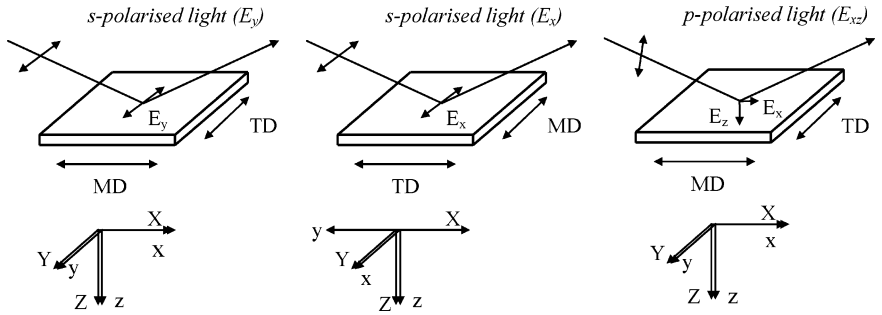

Figure 2. Setup for polarized light measurements on optically biaxial polymer films. The optical axes of the sample (*xyz*) are aligned with a Cartesian system of laboratory coordinates (*XYZ*).

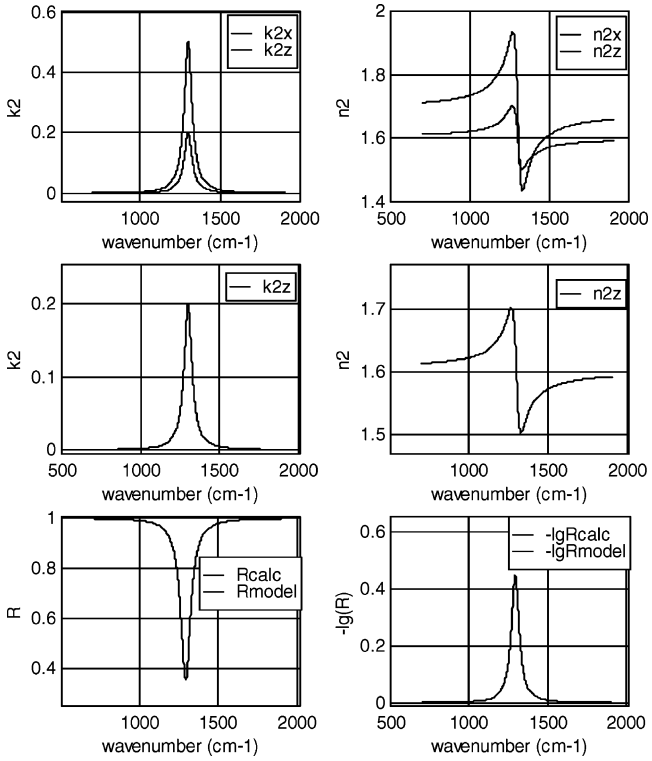

Figure 3. KK software validation using model ATR-IR peaks. Top row: optical constant spectra of a model anisotropic medium. The optical constants were created using the following parameters: $k_{2x\max,} = 0.5$, $n_{2x\infty} = 1.68$, $k_{2z\max} = 0.2$, $n_{2z\infty} = 1.6$, $\bar{\nu}_{\max} = 1300$ cm^{-1}. Middle row: results of the KK calculations performed on the model p-polarized light spectrum formed using the above optical constants, and assuming $n_1 = 4.0$ and $\theta_i = 30°$. Bottom row: model and calculated *R* spectra overlaid.

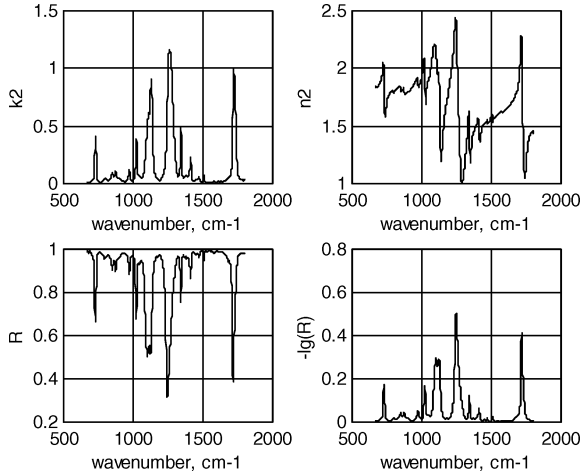

Figure 4. Results of the KK analysis performed on an ATR-IR spectrum of PET-T. The experimental conditions are as follows: s-polarization, $\theta_i = 40°$, $n_1 = 4.0$, $n_{2\infty} = 1.663$. The bottom row of the figure once more shows the experimental and calculated *R* spectra overlaid.

The validation of the code for extraction of optical constants was performed for both s- and p-polarized light on model spectra of different intensity in order to assess the accuracy of the code. In these calculations it was routinely possible to obtain values of less than 10^{-6} for the standard deviation $s = [(\sum_{\nu=1}^{N}(R_{\text{sim}} - R_{\text{calc}})^2)/(N - 1)]^{1/2}$, where N is the number of wavenumber points in the calculation. In general, most rapid convergence and highest accuracy were obtained for absorption bands of low and medium intensity. For absorption index spectra of $k_{2\max}$ greater than 0.5, the accuracy of the calculations decreased, and a greater number of iterations were required to reach the predetermined value of $s_{\min}$. The above is in line with a previous assessment of the accuracy of KK algorithms.[11]

In extracting optical constants from experimental spectra, there is the risk that noise or baseline distortion could be transferred into the calculated *n* and *k* spectra and lead to errors during concentration analysis. Poor spectral quality can also lead to instabilities during KK analysis. All ATR-IR experiments were therefore conducted very carefully in order to meet the stringent requirements for spectral quality. Purging the sample compartment with nitrogen allowed the collection of spectra with minimal noise. Baseline distortion was minimized by maintaining the spectrometer well aligned and optimizing the experimental conditions, e.g., sample alignment, applied force when clamping the sample in the ATR-IR accessory, etc. An example of the calculation of optical constants from the s-polarized light ATR-IR spectrum of a biaxially drawn PET film (PET-T) is given in Figure 4. Calculations in this particular example were stopped when the standard deviation reached a value of 5×10^{-5}. The latter was set as a target value for all calculations due to the fact that our earlier work on model spectra showed that the simulated optical constants were reproduced with sufficient accuracy when the standard deviation was brought to 10^{-4}–10^{-5}. The target value for the standard deviation was reached in most cases. Only in a small number of calculations where bands of high absorption intensity were present could the standard deviation not reach a value lower than 3×10^{-3}.

Optical Constants of PET. For most polymers including PET there is a lack of published optical constant standards. However, in quantitative ATR-IR work where spectral intensities depend strongly on the angle of incidence and on the refractive index of the ATR prism, verifying that experimental conditions are right

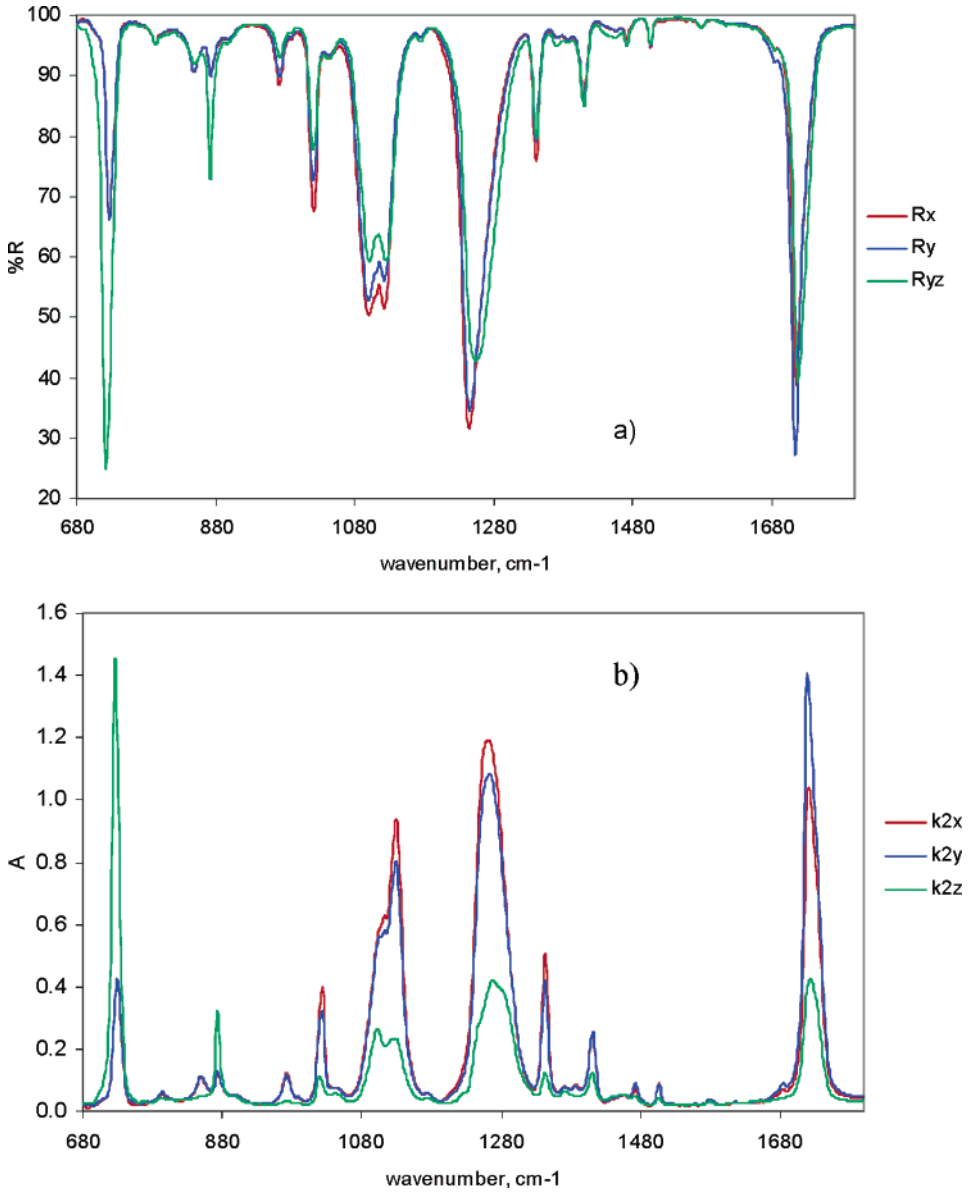

Figure 5. Polarized light analysis of biaxially drawn PET-T: (a) principal ATR-IR spectra, $n_1 = 4.0$, $\theta_i = 40°$; (b) the extracted principal absorption index spectra of PET-T. The inset to the figure shows the chemical structure of PET.

is only possible by subjecting the measured ATR-IR spectra to KK analysis and comparing the extracted n and k spectra with a standard. For a material the optical constants of which are unavailable, obtaining the standard n and k spectra is a necessary first stage of its quantitative spectroscopic analysis.

The ATR-IR analysis of PET with the purpose of establishing its optical constants was performed on a commercial film (PET-T) typical of that used in packaging. The film proved optically biaxial with principal refractive indices $n_{2\infty,x} = 1.663$, $n_{2\infty,y} = 1.645$, and $n_{2\infty,z} = 1.502$. The difference between the in-plane refractive indices $\Delta n_{2\infty,xy} = 0.018$ is small compared to $\Delta n_{2\infty,xz} = 0.161$ and $\Delta n_{2\infty,yz} = 0.143$, which shows that PET-T deviates only slightly from being optically uniaxial. This is according to expectations because films used in packaging usually undergo biaxial drawing with approximately equal draw ratios along MD and TD in order to obtain balanced properties in the plane of the film. We note that optically uniaxial films for which MD = TD ≠ ND are also termed "equibiaxial" by polymer scientists.

The ATR-IR spectra of PET-T are presented in Figure 5a. The p-polarized light spectrum (R_{yz}) differs significantly from the two s-polarized light spectra in the 900−680 cm^{-1} range. However, since the electric field of the incident light has components along both the in-plane (y) and the film normal direction (z), R_{yz} bears a lot of similarity with R_y in the rest of the spectral range. The difference in optical properties along the three macroscopic film directions is much more clearly demonstrated in Figure 5b, which shows the calculated absorption index spectra of the film. There, the k_x and k_y spectra are of a similar overall intensity. The intensity of most bands in the k_z spectrum range is about a third that of the in-plane spectra, with the exception of the two bands positioned at 873 and 726 cm^{-1}, which exhibit perpendicular dichroism. This result serves as further confirmation that despite a slight deviation from in-plane isotropy the optical properties of PET-T are well balanced in the in-plane direction.

Sample/ATR Crystal Contact. In Figure 5b it was tacitly assumed that the presented k spectra are the correct absorption index spectra of PET-T. It is however

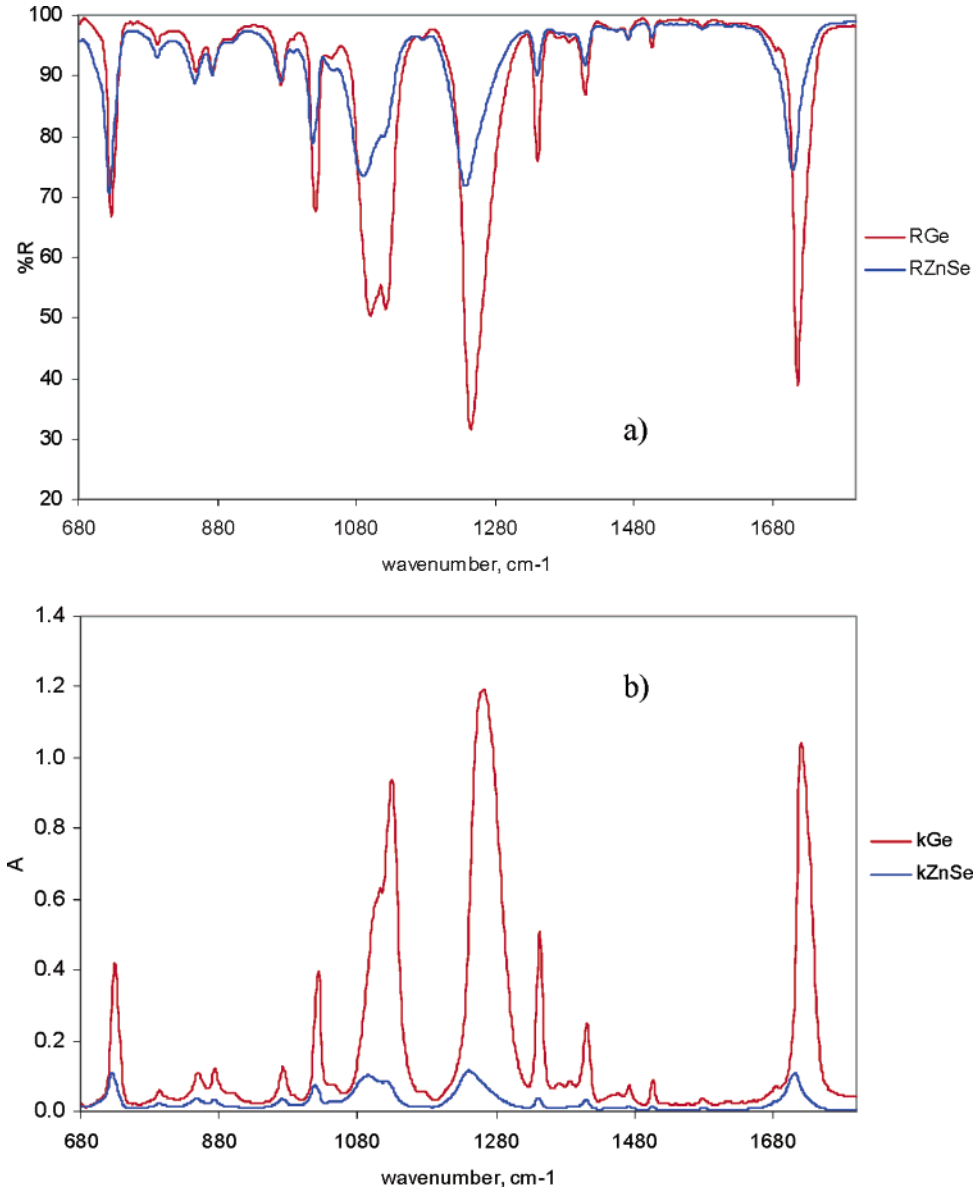

Figure 6. Influence of the sample/IRE contact on ATR-IR absorption intensity: (a) ATR-IR spectra of PET-T measured using ZnSe and Ge internal reflection elements; (b) absorption index spectra of PET-T calculated from the ATR-IR spectra shown above. The depths of penetration quoted in the text have been calculated at 1340 cm^{-1} using the following parameters: $\theta_{i,ZnSe} = 54°$, $n_{1,ZnSe} = 2.43$, $\theta_{i,Ge} = 40°$, $n_{1,Ge} = 4.0$, $n_2 = 1.663$.

well-known that one of the major drawbacks of ATR-IR spectroscopy is the difficulty in ensuring reproducible contact during measurements.

An example of what might go wrong in ATR-IR experiments is presented in Figure 6a. The figure contains the R curves of PET-T obtained using two different hemispherical ATR crystals, ZnSe and Ge. The attained depths of penetration (d_p) with the two IREs, calculated using the following expression[12]

$$d_p = \frac{\lambda}{2\pi(n_1^2 \sin^2 \theta_i - n_2^2)^{1/2}} \qquad (13)$$

are $d_{p1340}^{ZnSe} = 1.13$ μm and $d_{p1340}^{Ge} = 0.71$ μm. Since the amount of light absorbed by the medium is proportional to distance, the intensity of absorption peaks in the R_{ZnSe} spectrum should be greater than the intensity of absorption peaks in the R_{Ge} spectrum. In the example of Figure 6a, however, the opposite is true.

The discrepancy can be explained by taking into account that in FTIR work the sample spectrum is obtained by ratioing a sample spectrum to a background spectrum. To obtain the correct reflectivity spectrum, the contact area during the sample single-beam measurement should be equal to the area illuminated during the background measurement. When this requirement is not satisfied, the intensity of the absorption peaks in the reflectivity spectrum is lower than their true intensity. In the above example, the absorption intensity is greater in the spectrum obtained using a Ge hemispherical IRE because the latter acts as a surface of revolution of higher refractive power and hence shorter focal length than the ZnSe hemisphere. Light is therefore more focused at the sampling surface of the Ge crystal than at the sampling surface of the ZnSe crystal. Thus, better coverage of the illuminated area is achieved in the former case when the sample is clamped to the ATR crystal.

Figure 6b shows the k spectra of PET-T extracted from the reflectivity curves of Figure 6a. Clearly, depending on the experimental conditions in ATR-IR measurements the magnitude of the calculated optical

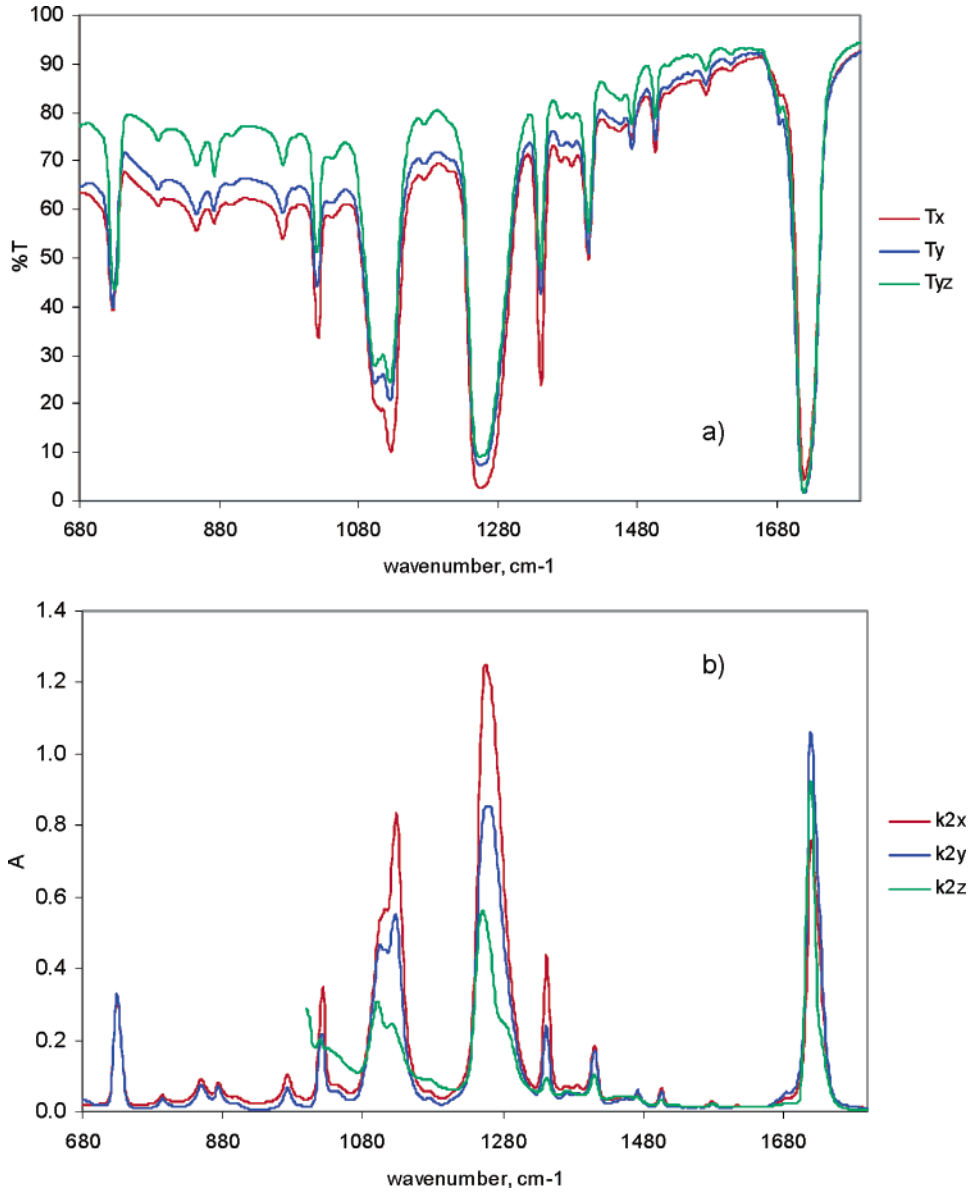

Figure 7. Polarized light analysis of PET-G: (a) principal ATR-IR spectra; (b) principal absorption index spectra. The (n, k) spectra were calculated using the following parameters: $\theta_i = 30°$, $n_1 = n_3 = 1.0$, $n_{2\infty,x} = 1.67$, $n_{2\infty,y} = 1.64$, $n_{2\infty,z} = 1.49$.

constants can vary substantially. Having realized the importance of the sample/IRE contact in quantitative ATR-IR analysis, it becomes mandatory to find out whether the optical constants of Figure 5b are correct and indeed establish a standard for future reference. Since the issue of adequate contact is always present in ATR-IR measurements, the magnitude of the optical constants of PET had to be further verified using transmission infrared spectroscopy.

PET-T being 12 μm thick proved unsuitable for transmission analysis. The film used for transmission work is PET-G (nominal thickness 1.5 μm). The polarized light spectra of PET-G measured along its principal axes are presented in Figure 7a. The optical constants of PET-G (Figure 7b) were extracted from its transmission spectra using the theory of wave propagation in stratified media.[3,5] During these calculations film thickness was adjusted from its nominal value of 1.5 μm to 1.75 μm in order to eliminate the presence of interference patterns in the derived absorption index spectra. As evident from Figure 7b, the extraction of the k_{2z} spectrum has not been entirely successful—calculations had to be restricted to a smaller wavenumber range due to the occurrence of instabilities. For the purpose of comparison of optical constants obtained by a contact and a noncontact method, however, the results of Figure 7b are satisfactory.

Figure 8 shows the structural factor spectra $k_0 = {}^1/_3(k_x + k_y + k_z)$ of PET-T and PET-G. The intensities of the two $k_{2,0}$ spectra derived from ATR-IR and transmission infrared measurements are remarkably similar. This proves that the contact between the PET-T film and the Ge crystal in the measurements of Figure 5 has been adequate. In view of this, all subsequent ATR-IR work was conducted using Ge as the incident medium without making additional changes in the experimental setup.

The "contact issue" is inherent to ATR-IR spectroscopy. In the words of Mirabella and Harrick,[13] the general use of this technique has been hampered by doubts about its reproducibility and capability to be quantitative. The last two works that have addressed the influence of sample/IRE contact in determining surface orientation in polymers are those of Mirabella[14]

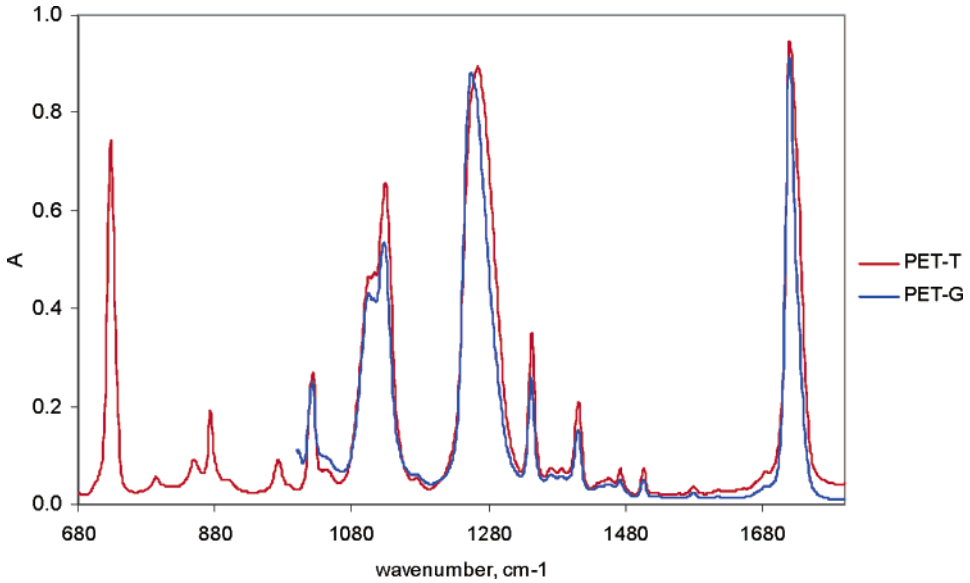

Figure 8. Structural factor spectra ($k_{2,0}$) of PET-T and PET-G.

and Everall and Bibby.[15] Mirabella[14] concluded that due to differing sample contact along the two in-plane sample directions only ATR−IR methods involving band ratios within a single spectrum can yield quantitative and reproducible orientation functions. In a similar fashion, Everall and Bibby[15] used normalization of band intensities relative to a nondichroic band prior to calculating dichroic ratios. According to the authors, normalization eliminates the need for maintaining identical contact areas when removing, rotating, and reclamping samples to the ATR crystal.

We note that in these works and in most previous literature on the subject the sample/IRE contact is treated in terms of its reproducibility or equality between measurements. In our work we have introduced the concept of contact adequacy. The phraseological difference between the two approaches may seem subtle, but the outcome of the two is very different. In the former case one is resigned to making measurements that do not yield the true reflectivity of the IRE/sample interface and looking for partial solutions in order to advance to "quantitative" analysis. In our contact adequacy approach contact reproducibility is not an issue. Contact adequacy is sought in order to (as discussed earlier in this section) measure correctly the reflectivity spectrum. Unless the correct reflectivity is obtained, the extraction of optical constants as a first stage of quantitative analysis becomes void of meaning. Since our analytical approach is methodologically rigorous, we have not had to use band normalization in the calculation of orientation functions. In contrast to Mirabella's and Everall and Bibby's experience, in our work band intensities from the principal absorption index spectra of PET (k_x, k_y, k_z) were directly employed in the analysis.[16]

Drawing Operations and Optical Anisotropy of Polymer Films. The extraction of optical constants of oriented polymers is not a well-established practice. In particular, we have not found examples in the literature where all three principal optical constant spectra of optically biaxial polymeric systems have been determined. It is therefore pertinent to examine the anisotropy of polymer films that have been subjected to a different number of drawing operations.

As shown in the previous section, the optical properties of the PET-T film, which has been drawn along two mutually orthogonal directions, are similar in the plane of the film but substantially different along its thickness direction. The film is therefore close to being optically uniaxial with the unique optic axis being oriented along the film thickness direction.

Below we examine the type of optical anisotropy exhibited by an amorphous PET film (PET-D) drawn in a nominally uniaxial-planar configuration. The PET-D film had some degree of preferred chain orientation but was able to partially relax when brought above its glass transition temperature in the grips of the Instron machine, before being drawn to a draw ratio $\lambda = 3.4$. The measured principal refractive indices of the drawn film $n_x = 1.652$, $n_y = 1.558$, and $n_z = 1.524$ and its polarized light ATR-IR spectra (Figure 9a) show that the resulting film possesses well-defined optical biaxiallity. The latter is further manifested in Figure 9b where the extracted absorption index spectra of the film are shown—all three k-spectra of the drawn PET-D film are very different in intensity. These results agree well with previous investigations of oriented PET,[17−20] which have shown that isotropic PET films subjected to uniaxial planar (constant width) deformation become optically biaxial.

It is important to note that in some cases the optical anisotropy of polymer films has been assigned on the basis of the number of drawing operations the films have endured; i.e., one-way drawn films have been treated as optically uniaxial,[21−23] and films formed by drawing along two orthogonal directions have been treated as optically biaxial.[22] In such analyses the optical properties of one-way drawn films are assumed equal along the transverse and thickness direction, whereas the optical properties of biaxially drawn films are assumed substantially different along all three film directions. The results on PET-T (Figure 5) and PET-D (Figure 9), however, clearly show that there is no equivalence between the number of drawing operations and the optical properties of polymer films. Therefore, when analyzing polymer films formed by tensile drawing, their anisotropy must be carefully examined in order to make sure that the subsequent use of spectro-

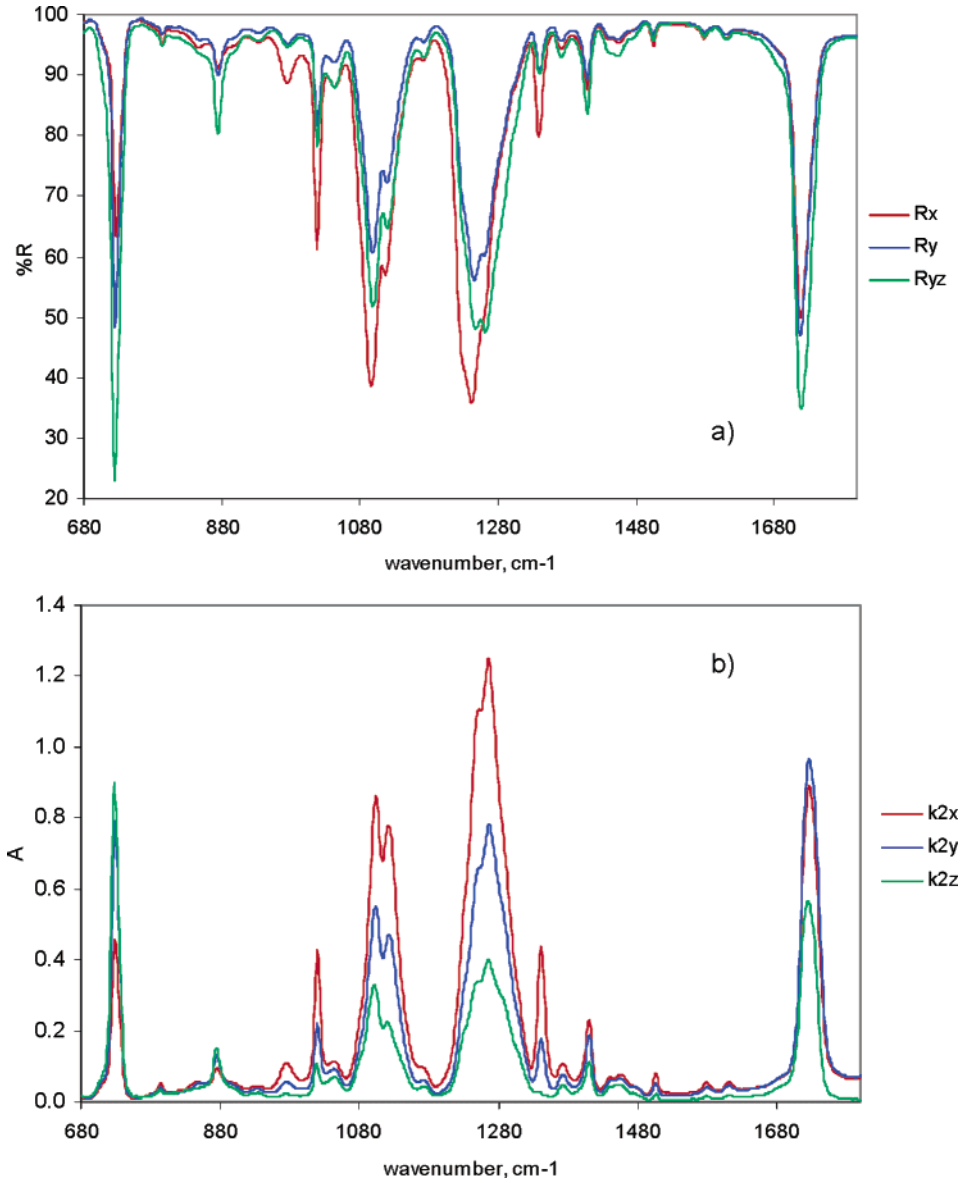

Figure 9. Polarized light analysis of the nominally uniaxially drawn PET-D film: (a) principal ATR-IR spectra, $\theta_i = 40°$, $n_1 = 4.0$; (b) principal absorption index spectra of PET-D.

scopic data for concentration and molecular orientation analysis is methodologically correct.

The anisotropy of polymer films can be foreseen if there is available information about the type of optical anisotropy exhibited by the polymer structural units, i.e., uniaxial or biaxial, and about the macroscopic orientation of polymer chains.[24] It is well established that tensile drawing of amorphous isotropic polymers leads to chain alignment along the direction of drawing. A one-way drawn polymer film composed of optically uniaxial microscopic units will therefore be optically uniaxial with the unique optic axis coinciding with the direction of drawing. If the microscopic constituent unit is optically biaxial, the macroscopic uniaxiallity of a one-way drawn polymer film must result from the random orientation of the structural units about their long chain axes. In the case in which the orientation about the long chain axes is not random, the film is bound to be optically biaxial.

In PET film production, the drawing of the amorphous and isotropic precursor material proceeds through a gauche/trans conformational change of the ethylene glycol (EG) residue and chain orientation of the monomer units containing *trans*-EG along the direction of drawing, followed by strain-induced crystallization. In Figure 9b, the absorptions located at 1340 and 971 cm^{-1} that are associated with the *trans*-EG conformer are very different in intensity in all three absorption index spectra. The same is true for the complex C−O bands centered about 1260 and 1100 cm^{-1} and for the 1018 cm^{-1} in-plane and 875 cm^{-1} out-of-plane benzene ring vibrations. The fact that the intensity of the 875 cm^{-1} band is greatest in the k_z spectrum shows that there is a preferential alignment of the benzene rings in the plane of the film. The orientation of the PET monomer units about their long axes is hence not random. The result of Figure 9b therefore provides strong evidence that PET monomer units containing EG segments in the trans conformation are optically biaxial.

Here we note that the classical models of the development of the photoelastic properties of deformed molecular networks[25−27] are based on the assumption of transverse polarizability isotropy. The use of such models in the analysis of the deformation of PET films

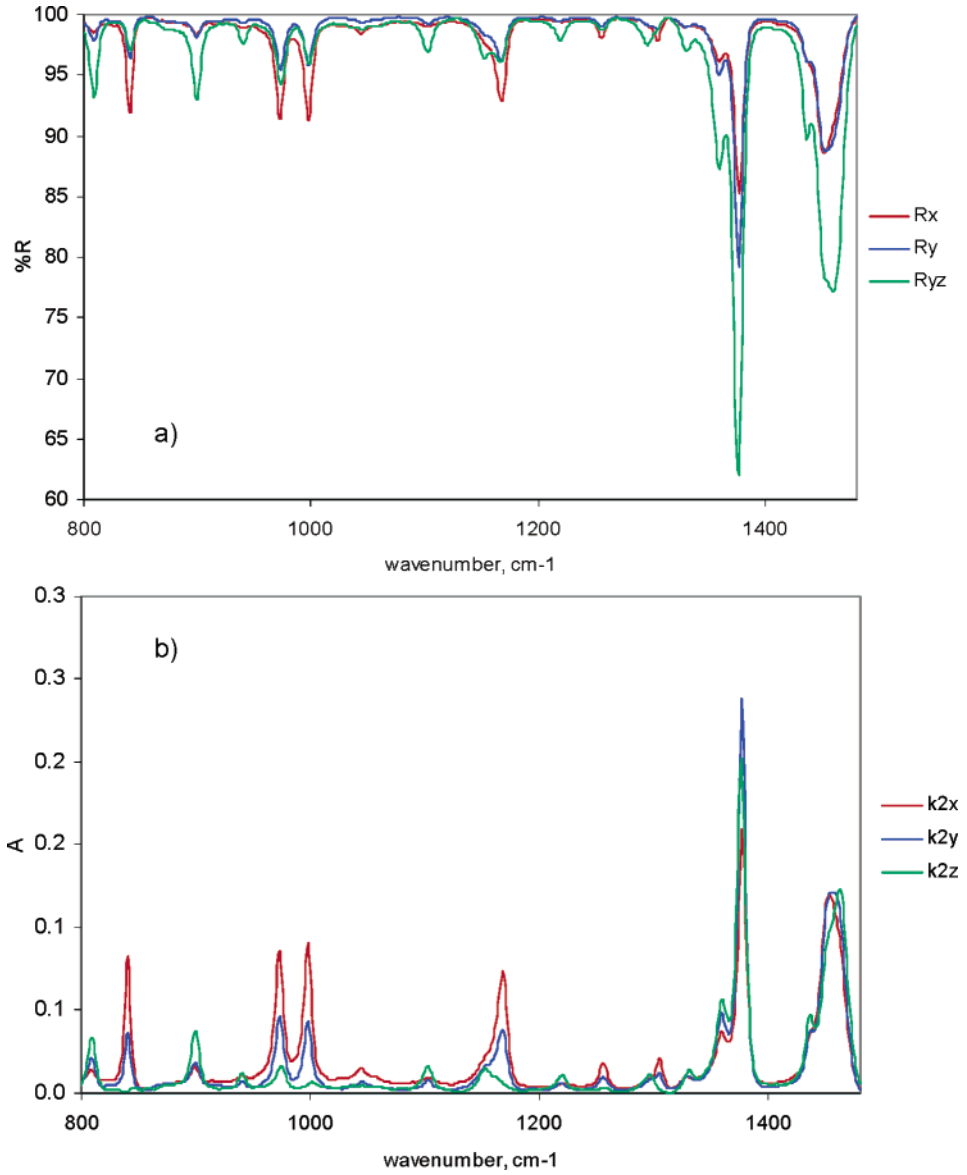

Figure 10. ATR-IR analysis of oriented polypropylene: (a) polarized ATR-IR spectra, $\theta_i = 32°$, $n_1 = 4.0$; (b) principal absorption index spectra.

therefore requires further refinement in order to account for the occurrence of a gauche−trans conformation change in PET during drawing.

Optical Constants and Degree of Crystallinity of OPP. The optical constants of polypropylene were extracted from the ATR-IR spectra of a commercial film. Infrared measurements made along several sample directions showed that the film is composed of isotactic polypropylene and that it has a direction of preferred chain orientation. The principal refractive indices of the film measured using an Abbe refractometer are $n_{2\infty,x} = 1.519$, $n_{2\infty,y} = 1.504$, and $n_{2\infty,z} = 1.499$. Despite the small refractive index differences, the film is clearly optically biaxial, and the application of the transverse isotropy approximation in its analysis is not appropriate. This is further corroborated by the polarized light ATR-IR spectra and the extracted principal absorption index spectra of the OPP film (Figure 10).

The intensities of the 998 and 973 cm^{-1} bands in the absorption coefficient (K_0) spectrum of the OPP film were used to estimate its degree of crystallinity in accord with a method suggested by Quynn et al.[28] The method is based on the linear relationship between the ratio of the 998 and 973 cm^{-1} bands and the density of isotactic polypropylene. The 998 cm^{-1} band arises from CH bending and CH_3 rocking vibrations of the regular helical structure of isotactic polypropylene whereas the 972 cm^{-1} is caused by coupled backbone C−C stretching and CH_3 rocking vibrations.[29] The estimated surface degree of crystallinity of the polypropylene film (ca. 80.5%) was found to be very similar to the degree of crystallinity of the bulk (ca. 80%) estimated from X-ray diffraction data. This result is in accord with previous comparisons of the surface and bulk structure of OPP films.[30,31]

Summary and Conclusions

We have employed the optical theory in the first stage of the quantitative ATR-IR analysis of anisotropic polymer films—the extraction of optical constants. Examples of optical constant extraction of PET were presented from which it is clear that unless care is taken to achieve adequate sample/ATR crystal contact, the intensity of absorption bands in the measured reflectivity spectra is diminished. As a result, the pair of n and k spectra calculated using KK analysis can be

substantially different from the true materials properties. Assessing contact adequacy however is difficult in the absence of optical constant standards. Contact adequacy in our experiments was proven by comparing the (n, k) spectra of PET calculated in the 1800−670 cm^{-1} range from ATR-IR and transmission infrared spectra. The optical constants of isotactic polypropylene in the 1400−800 cm^{-1} range were also presented.

We examined the type of optical anisotropy exhibited by PET films formed by one and two drawing operations. Uniaxial-planar PET films are strongly optically biaxial. In contrast, PET films formed by drawing to a similar draw ratio along two mutually orthogonal directions are close to being optically uniaxial—the optical properties are similar in the plane of the film but very different along the film thickness direction. The differences in optical anisotropy can be related to the difference in chain orientation induced during uniaxial-planar and biaxial deformation and to the anisotropy of the PET monomer unit. The example with PET films shows that the optical anisotropy of polymer films formed by tensile drawing cannot be assigned on the basis of the number of drawing operations. The anisotropy of such films must therefore be carefully examined in order to choose the right methodology in any subsequent concentration and molecular orientation analysis.

Acknowledgment. This work was funded by Toppan Printing Co. Ltd., Japan, and we gratefully acknowledge the contribution of Dr. Y. Tsukahara (Toppan Printing Co.) and Professor G. A. D. Briggs (Department of Materials, Oxford University) to it.

References and Notes

(1) Born, M.; Wolf, E. *Principles of Optics*, 6th ed.; Cambridge University Press: New York, 1998.
(2) Heavens, O. S. *Optical Properties of Thin Solid Films*, 3rd ed.; Dover Publications: New York, 1991.
(3) Fowles, G. R. *Introduction to Modern Optics*; Holt, Rinehart and Winston Inc.: New York, 1975.
(4) (Landau, L. D.; Lifshitz, F. M. *Electrodynamics of Continuous Media*; Pergamon: Oxford, 1960.
(5) Mosteller, L. P.; Wooten, F. *J. Opt. Soc. Am.* **1968**, *58*, 511.
(6) Bréhat, F.; Wyncke, B. *J. Phys. D* **1991**, *24*, 2205.
(7) Urban, M. *Attenuated Total Reflectance Spectroscopy of Polymers: Theory and Practice*; American Chemical Society: Washington, DC, 1996.
(8) Ribbegård, G. K.; Jones, R. N. *Appl. Spectrosc.* **1980**, *34*, 638.
(9) Ohta, K.; Ishida, H. *Appl. Spectrosc.* **1988**, *42*, 952.
(10) Bardwell, J. A.; Dignam, M. L. *J. Chem. Phys.* **1985**, *83*, 5468.
(11) Huang, J. B.; Urban, M. W. *Appl. Spectrosc.* **1992**, *46*, 1666.
(12) Harrick, N. J. *Internal Reflection Spectroscopy*; Interscience Publishers: New York, 1967.
(13) Mirabella, F. M.; Harrick, N. J. *Internal Reflection Spectroscopy: Review and Supplement*; Harrick Scientific Corp.: Ossining, NY, 1985.
(14) Mirabella, F. M. *Appl. Spectrosc.* **1988**, *42*, 1258.
(15) Everall, N. J.; Bibby, A. *Appl. Spectrosc.* **1997**, *51*, 1083.
(16) Kirov, K. R.; Assender, H. E. *Surface Structure of Anisotropic Polymer Films: Part II and III*, in preparation.
(17) Jarvis, D. A.; Hutchinson, I. J.; Bower, D. I.; Ward, I. M. *Polymer* **1980**, *21*, 41.
(18) Lapersonne, P.; Bower, D. I.; Ward, I. M. *Polymer* **1992**, *33*, 1266.
(19) Hutchinson, I. J.; Ward, I. M.; Willis, H. A.; Zichy, V. *Polymer* **1980**, *21*, 55.
(20) Everall, N. J.; Bibby, A. *Appl. Spectrosc.* **1997**, *51*, 1083.
(21) Cole, K. C.; Guèvremont, J.; Ajii, A.; Dumoulin, M. M. *Appl. Spectrosc.* **1994**, *48*, 1513.
(22) Cole, K. C.; Daly, H. B.; Sanschagrin, B.; Nguyen, K. T.; Ajii, A. *Polymer* **1999**, *40*, 3505.
(23) Lee, K.; Heeger, A. J. *Synth. Met.* **2002**, *128*, 279.
(24) Ward, I. M. *Adv. Polym. Sci.* **1985**, *66*, 81.
(25) Kratky, O. *Kolloidzeitschrift* **1930**, *64*, 213. Kuhn, W.; Grün, F. *Kolloidzeitschrift* **1942**, *101*, 248; in Ward, I. M., Ed., *Structure and Properties of Oriented Polymers*, 2nd ed.; Chapman and Hall: New York, 1997.
(26) Treloar, L. R. G. *The Physics of Rubber Elasticity*; Clarendon Press: Oxford, 1975.
(27) Treloar, L. R. G.; Riding, G. *Proc. R. Soc. London A* **1979**, 281.
(28) Quynn, R. G.; Riley, J. L.; Young, D. A.; Noether, H. D. *J. Appl. Polym. Sci.* **1959**, *2*, 166.
(29) Bower, D. I.; Maddams, W. F. *The Vibrational Spectroscopy of Polymers*; Cambridge University Press: New York, 1989.
(30) Hobbs, J. P.; Sung, C. S. P.; Krishnan; Hill, S. *Macromolecules* **1983**, *16*, 193.
(31) Mirabella, F. M., Jr. *J. Polym. Sci., Part B* **1984**, *22*, 1293.

MA030369J